

Realistic indirect spin-interactions between magnetic impurities on a metallic Pb(110) surface

Alejandro Rébola¹ and Alejandro M. Lobos^{2,3}

¹*Instituto de Física Rosario - CONICET, Bv. 27 de Febrero 210 bis, 2000 Rosario, Argentina**

²*Facultad de Ciencias Exactas y Naturales Universidad Nacional de Cuyo, 5500 Mendoza, Argentina*

³*Consejo Nacional de Investigaciones Científicas y Técnicas (CONICET), Argentina*

Motivated by recent experiments, here we study the indirect interactions between magnetic impurities deposited on top of a clean Pb(110) surface induced by the underlying conduction electrons. Our approach makes use of *ab initio* calculations to characterize the clean Pb(110) surface and avoids self-consistency, a feature that greatly reduces the computational cost. In combination with 2nd order perturbation theory in the microscopic *s-d* exchange parameter J_K between a magnetic adatom and the conduction electrons, we are able to systematically derive the Ruderman-Kittel-Kasuya-Yosida (RKKY), the Dzyaloshinskii-Moriya (DM) and the anisotropic tensor interactions emerging at the Pb(110) surface between magnetic impurities. The only adjustable parameter is J_K , which is fitted to reproduce the experiments. Our results show important anisotropy effects arising both from the rectangular geometry of the (110) unit cell, and from the strong Rashba spin-orbit interaction due to the broken inversion symmetry at the Pb(110) surface. In addition to Pb(110), the characterization of the indirect spin interactions described here could be extended to other realistic metallic surfaces for weakly-coupled impurities, and would enable to fabricate atomic-size nanostructures with engineered interactions and on-demand magnetic properties, anticipating useful applications in nanotechnology.

I. INTRODUCTION

The Rudermann-Kittel-Kasuya-Yosida (RKKY) exchange interaction is an indirect magnetic coupling between localized magnetic moments, mediated by the conduction electrons in a metallic substrate¹⁻³. This type of interaction plays a crucial role in systems displaying giant magnetoresistance⁴, heavy-fermion magnetism and quantum criticality⁵⁻⁷, and in dilute magnetic semiconductors^{8,9}. More recently, it has also been observed in atomic-scale magnetic systems fabricated with scanning tunneling microscopy (STM) techniques¹⁰⁻¹⁵. In these atomic-sized structures the RKKY interaction plays a major role. For instance, it has been recently proposed as a key ingredient in magnetic atomic chains deposited on conventional superconductors with a strong Rashba spin-orbit coupling (SOC), systems predicted to host Majorana-fermion quasiparticles (MQP)¹⁶⁻¹⁸. These works have triggered a great amount of theoretical and experimental research seeking to observe MQPs, which could be instrumental in the fabrication of qubits for topological quantum computers. In recent experimental works involving atomic Fe chains on top of clean Pb(111) or Pb(110) surfaces, preliminar evidence of MQPs have been reported¹⁹⁻²².

Assuming an idealized isotropic free-electron conduction band, the standard result for the RKKY interaction is $J_{\text{RKKY}}(\mathbf{r}) \sim \cos(k_F r)/r^D$, where k_F the Fermi momentum and $r = |\mathbf{r}|$ the distance between the magnetic impurities is obtained¹⁻³. However, the behavior of real adatom systems on metallic surfaces is strikingly different, and departures from an ideally isotropic interaction has been reported experimentally. For instance, one of the most relevant results in the abovementioned Refs. 10-12, and 15 is the anisotropic character of the RKKY

interaction on surfaces. Considering the growing interest in the fabrication of magnetic devices with specific functionalities and potential applications in quantum computing, spintronic and magnetic memories, a detailed characterization of realistic magnetic interactions would be highly desirable. From a more fundamental perspective, a realistic characterization of the RKKY interaction on specific metallic surfaces could also be useful to simulate, in a controlled manner, the physics of strongly-correlated materials. For instance, using self-assembled metal-organic networks deposited on clean metallic surfaces, a controlled study of the celebrated Kondo lattice model, typically used to understand the exotic low-temperature behavior of heavy-fermion materials, has become possible with STM techniques²³⁻²⁵.

Among the many possible metallic surfaces typically studied with STM, the surface of Pb has become an ideal platform to study the interplay between superconductivity and atomic magnetism. The interest is two-fold: 1) Pb becomes a conventional *s*-wave superconductor at low temperatures, with a standard phonon-mediated pairing mechanism. In addition, its relative simplicity to grow in films by evaporation techniques makes it a widely used superconducting material in the laboratory. 2) A large Rashba SOC exists at the surface of Pb, a property that is known to induce large Dzyaloshinskii-Moriya interactions. This property could be exploited in order to engineer non-colinear chiral magnetic nanostructures, such as skyrmions^{14,26}. Both features could prove extremely useful in novel spintronic devices²⁷⁻³¹. In previous works, perturbative approaches combined with numerical and/or semi-analytical methods for realistic band-structure calculations have been used for the calculation of the RKKY indirect-exchange interaction between nuclear moments³²⁻³⁵. However, none of these

works have focused on magnetic impurities on Pb, where relativistic effects are unavoidable. On the other hand, the calculation of the Dzyaloshinskii-Moriya interaction has been tackled in previous works using highly idealized model Hamiltonians^{26,36–38}, which ignore the real electronic structure. Therefore, there are no systematic studies of the realistic magnetic interactions on the surface of Pb.

Motivated by the aforementioned experimental advances, in this article we focus on the derivation of realistic magnetic interactions between impurities on top of a clean Pb surface. For concreteness, and in order to make contact with Refs. 19–22, we have chosen the particular case of Pb(110) surface. However, we stress that our method is also applicable to other systems. Using a combination of an analytical approach, i.e., second-order perturbation theory in the s - d exchange interaction J_K , and density functional theory (DFT) to obtain the full band structure of Pb(110) including relativistic SOC effects, we systematically derive the RKKY, the Dzyaloshinskii-Moriya (DM) and the anisotropic tensor interactions between magnetic impurities. Our results show important anisotropy effects arising both from the rectangular geometry of the (110) unit cell, and from the strong Rashba SOC originated in the broken inversion symmetry at the Pb(110) surface.

Since within our perturbative approach only the band structure of the *clean* Pb(110) surface is needed, the computational cost can be significantly reduced. This represents one of the main advantages of our method: the possibility to describe indirect magnetic interactions realistically (i.e., without having to resort to any *a priori* model or approximation), combined with low computational cost as compared to standard self-consistent methods, such as the Korringa-Kohn-Rostoker (KKR) method. Due to the nature of the method, its applicability is in principle limited to weakly-coupled adatom systems satisfying the condition $\rho_{3D}J_K \ll 1$, where ρ_{3D} is the density of conduction states per unit volume at the Fermi energy. Such limitation is, nevertheless, not severe as there exist many examples of systems fulfilling this condition [e.g., metal-organic complexes such as MnPc molecules³⁹ or iron(II) porphyrin molecules⁴⁰ deposited on top of Pb(110), where the organic ligand of the molecule tends to isolate the effective magnetic moment from the surface, leading to a small effective coupling J_K]. The only adjustable parameter in our formalism is therefore the s - d exchange parameter J_K , which is fitted to reproduce experiments³⁹.

The rest of the paper is organized as follows. In Sec. II we present the theoretical model and the derivation of the generic RKKY, DM and tensor interactions directly from the conduction-electron propagators. In Sec. III we give details about the technical aspects of the *ab initio* calculations and about the convergence of the RKKY interaction. In Sec. IV we present the results, specifically in Sec. IV A we present our results for the band-structure of the clean Pb(110), and in Sec. IV C we show our re-

sults for the magnetic RKKY, DM and tensor interactions. Finally, in Sec. V we summarize the main results and present the conclusions.

II. THEORETICAL MODEL AND DERIVATION OF THE EFFECTIVE INTERACTIONS

The theoretical model describing two spin impurities on a Pb(110) surface, located at sites $\mathbf{r}_1 = (x_1, y_1, 0)$ and $\mathbf{r}_2 = (x_2, y_2, 0)$ where $z = 0$ is the coordinate of the surface plane, is

$$H = H_0 + H_K(1) + H_K(2). \quad (1)$$

Here

$$H_0 = \sum_{\mathbf{k},n} \epsilon_{\mathbf{k},n}^{(0)} c_{\mathbf{k},n}^\dagger c_{\mathbf{k},n}, \quad (2)$$

is the unperturbed Hamiltonian describing the bands of clean Pb(110). The quantum numbers \mathbf{k}, n are, respectively, the crystal momentum parallel to the surface belonging to the first Brillouin zone, and the spin-orbital band index, which results from a combination of the spin and the azimuthal angular momentum (recall that in the presence of Rashba and/or Dresselhaus SOC, s , the spin projection along z is no longer a good quantum number. In the absence of Rashba SOC, the index n splits into s and the usual band index α). The operator $c_{\mathbf{k},n}$ annihilates a fermionic quasiparticle in the conduction band, and obeys the usual anticommutation relation $\{c_{\mathbf{k},n}, c_{\mathbf{k}',n'}^\dagger\} = \delta_{\mathbf{k},\mathbf{k}'} \delta_{n,n'}$. Finally, $\epsilon_{\mathbf{k},n}^{(0)}$ is the dispersion relation computed in the absence of the magnetic impurities.

The Kondo (or s - d exchange) interaction between a magnetic moment and the conduction-electron spin density at point \mathbf{r}_j is⁶

$$H_K(j) = J_K \mathbf{S}_j \cdot \mathbf{s}(\mathbf{r}_j) \quad (3)$$

$$= J_K \mathbf{S}_j \cdot \sum_{s,s'=\{\uparrow,\downarrow\}} \Psi_s^\dagger(\mathbf{r}_j) \left(\frac{\hat{\boldsymbol{\sigma}}}{2} \right)_{ss'} \Psi_{s'}(\mathbf{r}_j), \quad (4)$$

where $\hat{\boldsymbol{\sigma}} = (\hat{\sigma}_x, \hat{\sigma}_y, \hat{\sigma}_z)$ is the vector of Pauli matrices, and

$$\Psi_s(\mathbf{r}_j) = \sum_{\mathbf{k},n} \psi_{\mathbf{k},n}^{(s)}(\mathbf{r}_j) c_{\mathbf{k},n}, \quad (5)$$

is the field operator which annihilates an electron with spin projection $s = \{\uparrow, \downarrow\}$ along the z axis at point \mathbf{r}_j , and $\psi_{\mathbf{k},n}^{(s)}(\mathbf{r})$ are the normalized Bloch wavefunctions computed via DFT (see Section III). The field operator obeys the usual relations:

$$\sum_{\mathbf{k},n} \psi_{\mathbf{k},n}^{*(s)}(\mathbf{r}_i) \psi_{\mathbf{k},n}^{(s')}(\mathbf{r}_j) = \delta(\mathbf{r}_i - \mathbf{r}_j) \delta_{s,s'}, \quad (6)$$

$$\{\Psi_s(\mathbf{r}_i), \Psi_{s'}^\dagger(\mathbf{r}_j)\} = \delta(\mathbf{r}_i - \mathbf{r}_j) \delta_{s,s'}. \quad (7)$$

The idea now is to use knowledge of the *realistic* band structure of Pb(110), encoded in $\epsilon_{\mathbf{k},n}^{(0)}$ and $\psi_{\mathbf{k},n}^{(s)}(\mathbf{r}_j)$, in order to systematically derive all the effective interactions between \mathbf{S}_1 and \mathbf{S}_2 mediated by the conduction electrons using second-order perturbation theory in J_K , and without resorting to any specific model. In the process, not only the RKKY exchange is obtained, but also Dzyaloshinskii-Moriya and anisotropic tensor interactions.

We start from the full partition function of the system, which formally writes as

$$Z = \text{Tr} \left\{ e^{-\beta(H_0 + \sum_j H_K(j))} \right\},$$

$$= \text{Tr}_S \text{Tr}_\psi \left\{ e^{-\beta(H_0 + \sum_j H_K(j))} \right\}, \quad (8)$$

where $\beta = 1/T$ (here we have assumed $k_B = 1$). In Eq. (8) we have split the total trace into partial traces over fermionic (noted as Tr_ψ) and spin (noted as Tr_S) degrees of freedom. This allows to define the quantity $Z_S \equiv \text{Tr}_\psi \left\{ e^{-\beta(H_0 + \sum_j H_K(j))} \right\}$, where the partial trace over the electrons is taken considering a particular “frozen” configuration of the spins \mathbf{S}_1 and \mathbf{S}_2 . In the zero-temperature limit $\beta \rightarrow \infty$, this quantity allows to define an effective spin Hamiltonian where the electronic degrees of freedom have been integrated out

$$Z_S = e^{-\beta H_{\text{eff}}[\mathbf{S}_1, \mathbf{S}_2]} \quad (\text{for } \beta \rightarrow \infty). \quad (9)$$

Using the path-integral formalism⁴¹, Z_S can be expressed as

$$Z_S = \int \mathcal{D}[\bar{c}, c] e^{-S_0[\bar{c}, c] - \sum_j S_{K,j}[\mathbf{S}_j, \bar{c}, c]},$$

where \bar{c}, c are Grassmann variables and $S_0[\bar{c}, c]$ and $S_{K,j}[\mathbf{S}_j, \bar{c}, c]$ are, respectively

$$S_0[\bar{c}, c] = \sum_{\mathbf{k}, n} \int_0^\beta d\tau \bar{c}_{\mathbf{k}, n}(\tau) \left(\partial_\tau - \epsilon_{\mathbf{k}, n}^{(0)} \right) c_{\mathbf{k}, n}(\tau), \quad (10)$$

the Euclidean action of the unperturbed Pb(110), expressed as an integral over Matsubara time τ in the interval $[0, \beta]$, and

$$S_{K,j}[\mathbf{S}_j, \bar{c}, c] = J_K \mathbf{S}_j \sum_{s, s'} \int_0^\beta d\tau \Psi_s^\dagger(\mathbf{r}_j, \tau) \frac{\hat{\sigma}_{ss'}}{2} \Psi_{s'}(\mathbf{r}_j, \tau), \quad (11)$$

is the Euclidean action of the s - d interaction. The advantage of the path-integral formalism is that it allows to express Z_S as a series expansion in powers of J_K as

$$Z_S = Z_0 \sum_{m=0}^{\infty} \frac{1}{m!} \left\langle \left(\sum_j S_{K,j}[\mathbf{S}_j, \bar{c}, c] \right)^m \right\rangle_0, \quad (12)$$

where the notation $\langle A \rangle_0$ means the average of operator A with respect to the action S_0 , i.e., $\langle A \rangle_0 =$

$\int \mathcal{D}[\bar{c}, c] e^{-S_0[\bar{c}, c]} A_0 / Z_0$, with $Z_0 = \int \mathcal{D}[\bar{c}, c] e^{-S_0[\bar{c}, c]}$ the partition function of unperturbed electrons in Pb(110).

The above Eqs. (8)-(12) are formally exact, but in order to make progress we need to introduce a truncation in the infinite series in Eq. (12), assuming $J_K \rightarrow 0$. At second order, and introducing a subsequent cumulant expansion⁴², the quantity Z_S can be approximated as

$$Z_S \approx e^{\frac{1}{2} \langle (S_{K,1}[\mathbf{S}_1, \bar{c}, c] + S_{K,2}[\mathbf{S}_2, \bar{c}, c])^2 \rangle_0}, \quad (13)$$

(note that the first order term in (12) has vanished due to the time-reversal symmetry of the Pb(110) conduction band). Comparing Eqs. (9) and (13), we obtain the precise analytical form for the effective spin Hamiltonian at second order in J_K :

$$H_{\text{eff}}[\mathbf{S}_1, \mathbf{S}_2] = -\frac{1}{2\beta} \lim_{\beta \rightarrow \infty} \left\langle (S_{K,1}[\mathbf{S}_1, \bar{c}, c] + S_{K,2}[\mathbf{S}_2, \bar{c}, c])^2 \right\rangle_0, \quad (14)$$

where the conduction-electrons of the Pb(110) band has been integrated out. The effective Hamiltonian can be expressed as

$$H_{\text{eff}}[\mathbf{S}_1, \mathbf{S}_2] = \lim_{\beta \rightarrow \infty} \frac{J_K^2}{8} \frac{1}{\beta} \sum_l \sum_{i,j=1,2} \text{tr} \{ (\mathbf{S}_i \cdot \hat{\sigma}) \hat{\mathbf{g}}_0(\mathbf{r}_i, \mathbf{r}_j, i\nu_l) (\mathbf{S}_j \cdot \hat{\sigma}) \hat{\mathbf{g}}_0(\mathbf{r}_j, \mathbf{r}_i, i\nu_l) \}, \quad (15)$$

where $\text{tr}\{\dots\}$ is the usual trace of a matrix, and $\hat{\mathbf{g}}_0(\mathbf{r}_i, \mathbf{r}_j, i\nu_l)$ is the matrix of the unperturbed conduction-electron propagators in Pb(110)

$$\hat{\mathbf{g}}_0(\mathbf{r}_i, \mathbf{r}_j, i\nu_l) = \begin{pmatrix} g_0^{(\uparrow\uparrow)}(\mathbf{r}_j, \mathbf{r}_i, i\nu_l) & g_0^{(\uparrow\downarrow)}(\mathbf{r}_j, \mathbf{r}_i, i\nu_l) \\ g_0^{(\downarrow\uparrow)}(\mathbf{r}_j, \mathbf{r}_i, i\nu_l) & g_0^{(\downarrow\downarrow)}(\mathbf{r}_j, \mathbf{r}_i, i\nu_l) \end{pmatrix}, \quad (16)$$

with matrix elements

$$g_0^{(ss')}(\mathbf{r}_j, \mathbf{r}_i, i\nu_l) = \sum_{\mathbf{k}, n} \frac{\psi_{\mathbf{k}, n}^{(s)}(\mathbf{r}_j) \psi_{\mathbf{k}, n}^{*(s')}(\mathbf{r}_i)}{i\nu_l - \epsilon_{\mathbf{k}, n}^{(0)}} \quad (s, s' = \{\uparrow, \downarrow\}). \quad (17)$$

In this expression we have introduced the fermionic Matsubara frequencies $i\nu_l = 2\pi i(l + \frac{1}{2})/\beta$. Physically, the Green's function $g_0^{(ss')}(\mathbf{r}_j, \mathbf{r}_i, i\nu_l)$ measures the probability that an electron created at \mathbf{r}_i with spin s' arrives at \mathbf{r}_j with spin s in the unperturbed surface of Pb(110). Note that in absence of SOC, the spin-projection labels s and s' would be good quantum numbers and therefore the off-diagonal elements would vanish. Moreover, due to the SU(2) symmetry in the absence of SOC and externally applied magnetic fields, $g_0^{(\uparrow\uparrow)}(\mathbf{r}_j, \mathbf{r}_i, i\nu_l) = g_0^{(\downarrow\downarrow)}(\mathbf{r}_j, \mathbf{r}_i, i\nu_l)$ and therefore the matrix $\hat{\mathbf{g}}_0(\mathbf{r}_i, \mathbf{r}_j, i\nu_l)$ would be a scalar proportional to the unit matrix. In

what follows, we introduce a more convenient representation of the propagator matrix (16) in terms of the 2×2 Pauli matrices⁴³

$$\hat{\mathbf{g}}_0(\mathbf{r}_i, \mathbf{r}_j, i\nu_l) = g_0^0(\mathbf{r}_i, \mathbf{r}_j, i\nu_l) \mathbf{1}_{2 \times 2} + g_0^x(\mathbf{r}_i, \mathbf{r}_j, i\nu_l) \hat{\sigma}_x + g_0^y(\mathbf{r}_i, \mathbf{r}_j, i\nu_l) \hat{\sigma}_y + g_0^z(\mathbf{r}_i, \mathbf{r}_j, i\nu_l) \hat{\sigma}_z, \quad (18)$$

where the new propagators $g_0^k(\mathbf{r}_i, \mathbf{r}_j, i\nu_l)$ (with $k = \{0, x, y, z\}$) are linear combinations of the propagators (17), which allow to readily evaluate the trace in Eq.(15), and express the Hamiltonian as

$$H_{\text{eff}}[\mathbf{S}_1, \mathbf{S}_2] = J_{\text{RKKY}}(\mathbf{r}_1, \mathbf{r}_2) \mathbf{S}_1 \cdot \mathbf{S}_2 + \mathbf{D}_{\text{DM}}(\mathbf{r}_1, \mathbf{r}_2) \cdot (\mathbf{S}_1 \times \mathbf{S}_2) + 2\mathbf{S}_1 \cdot \mathbf{T}(\mathbf{r}_1, \mathbf{r}_2) \cdot \mathbf{S}_2 + \mathbf{S}_1 \cdot \mathbf{T}(\mathbf{r}_1, \mathbf{r}_1) \cdot \mathbf{S}_1 + \mathbf{S}_2 \cdot \mathbf{T}(\mathbf{r}_2, \mathbf{r}_2) \cdot \mathbf{S}_2. \quad (19)$$

Here we have defined the scalar RKKY exchange-interaction as

$$J_{\text{RKKY}}(\mathbf{r}_1, \mathbf{r}_2) = \frac{J_K^2}{2} \frac{1}{\beta} \sum_l \left[g_0^0(\mathbf{r}_1, \mathbf{r}_2, i\nu_l) g_0^0(\mathbf{r}_2, \mathbf{r}_1, i\nu_l) - \sum_{j=\{x,y,z\}} g_0^j(\mathbf{r}_1, \mathbf{r}_2, i\nu_l) g_0^j(\mathbf{r}_2, \mathbf{r}_1, i\nu_l) \right], \quad (20)$$

The next term in Eq. (19) corresponds to the Dzyaloshinskii-Moriya interaction

$$D_{\text{DM}}^j(\mathbf{r}_1, \mathbf{r}_2) = i \frac{J_K^2}{2} \frac{1}{\beta} \sum_l \left[g_0^0(\mathbf{r}_1, \mathbf{r}_2, i\nu_l) g_0^j(\mathbf{r}_2, \mathbf{r}_1, i\nu_l) - g_0^j(\mathbf{r}_1, \mathbf{r}_2, i\nu_l) g_0^0(\mathbf{r}_2, \mathbf{r}_1, i\nu_l) \right] \quad (j = \{x, y, z\}), \quad (21)$$

which is an anisotropic vector interaction. Finally, the last terms are anisotropic tensor interactions of the form

$$T^{jk}(\mathbf{r}_1, \mathbf{r}_2) = \frac{J_K^2}{4} \frac{1}{\beta} \sum_l \left[g_0^j(\mathbf{r}_1, \mathbf{r}_2, i\nu_l) g_0^k(\mathbf{r}_2, \mathbf{r}_1, i\nu_l) + g_0^j(\mathbf{r}_2, \mathbf{r}_1, i\nu_l) g_0^k(\mathbf{r}_1, \mathbf{r}_2, i\nu_l) \right], \quad (j, k = \{x, y, z\}) \quad (22)$$

which generalize the Ising and the single-ion magneto-crystalline contributions. Note that in (19) we have neglected the RKKY self-interaction terms

$J_{\text{RKKY}}(\mathbf{r}_j, \mathbf{r}_j) \mathbf{S}_j^2$, since they are only a renormalization of the energy.

Although the three contributions Eqs. (20)-(22) are of the same order $\mathcal{O}(J_K^2)$, their relative magnitude strongly depends on the magnitude of the Rashba SOC parameter α_R . This can be understood directly at the level of the propagators $g_0^{(x,y)}(\mathbf{r}_1, \mathbf{r}_2, i\nu_l)$ appearing in these expressions, which are directly proportional to the SU(2) symmetry-breaking terms in the Hamiltonian, as shown in previous works^{26,43}. Then, it is easy to see that

$$J_{\text{RKKY}}(\mathbf{r}_1, \mathbf{r}_2) \sim \mathcal{O}(1), \\ |\mathbf{D}_{\text{DM}}(\mathbf{r}_1, \mathbf{r}_2)| \sim \mathcal{O}(\alpha_R), \\ \|\mathbf{T}(\mathbf{r}_1, \mathbf{r}_2)\| \sim \mathcal{O}(\alpha_R^2),$$

III. METHODS AND TECHNICAL CONSIDERATIONS

A technical point in the derivation of the RKKY interaction Eq. (20) concerns the sum over the band index n , whose convergence is very slow. In principle, this sum runs over an infinite number of bands, but in practice must be limited by a cutoff energy E_c that ensures the convergence of the involved quantities. Due to its poor convergence properties, for a reasonable accuracy in the value of $J_{\text{RKKY}}(\mathbf{r}_1, \mathbf{r}_2)$ an unfeasible large value of E_c would be necessary (even for values of the order of $E_c = 100$ eV, errors would still be over 100%). However, it is physically expected that above a certain E_c the system wavefunctions are indistinguishable from the corresponding free-electron wavefunctions at the same energy. In other words, at sufficiently high energies $\epsilon_{\mathbf{k},n}^{(0)}$, it is expected that

$$\epsilon_{\mathbf{k},n}^{(0)} \approx \epsilon_{\mathbf{k}}^{\text{free}} = \frac{\hbar^2 (\mathbf{k} + \mathbf{G}_n)^2}{2m}, \quad (23)$$

$$\psi_{\mathbf{k}n}^{(s)}(\mathbf{r}) \approx \frac{e^{i(\mathbf{k} + \mathbf{G}_n) \cdot \mathbf{r}}}{\sqrt{V}}, \quad (24)$$

with \mathbf{G}_n a reciprocal-lattice vector. Taking this into account, the RKKY exchange interaction Eq. (20) at $T = 0$ can then be recast as

$$J_{\text{RKKY}}(\mathbf{r}_1, \mathbf{r}_2) = J_{\text{RKKY}}^0(\mathbf{r}_1, \mathbf{r}_2) + J_{\text{RKKY}}^{\text{free}}(\mathbf{r}_1, \mathbf{r}_2), \quad (25)$$

where

$$J_{\text{RKKY}}^0(\mathbf{r}_1, \mathbf{r}_2) = \frac{J_K^2}{4} \sum_{s=\{\uparrow, \downarrow\}} \sum_{\mathbf{k}, n}^{\epsilon_{\mathbf{k}n} < E_F} \times \frac{1}{V} \sum_{\mathbf{k}', n'}^{\substack{E_F < \epsilon_{\mathbf{k}'n'} < E_c \\ \epsilon_{\mathbf{k}n}^{(0)} - \epsilon_{\mathbf{k}'n'}^{(0)}}} \frac{1}{\epsilon_{\mathbf{k}n}^{(0)} - \epsilon_{\mathbf{k}'n'}^{(0)}} \times \left[\psi_{\mathbf{k}n}^{(s)}(\mathbf{r}_1) \psi_{\mathbf{k}n}^{*(s)}(\mathbf{r}_2) \psi_{\mathbf{k}'n'}^{(\bar{s})}(\mathbf{r}_2) \psi_{\mathbf{k}'n'}^{*(\bar{s})}(\mathbf{r}_1) - \psi_{\mathbf{k}n}^{(s)}(\mathbf{r}_1) \psi_{\mathbf{k}n}^{*(\bar{s})}(\mathbf{r}_2) \psi_{\mathbf{k}'n'}^{(\bar{s})}(\mathbf{r}_2) \psi_{\mathbf{k}'n'}^{*(s)}(\mathbf{r}_1) \right], \quad (26)$$

$$J_{\text{RKKY}}^{\text{free}}(\mathbf{r}_1, \mathbf{r}_2) = \frac{J_K^2}{4} \sum_{s=\{\uparrow, \downarrow\}} \sum_{\mathbf{k}, n}^{\epsilon_{\mathbf{k}n} < E_F} \frac{1}{V} \sum_{\mathbf{k}'}^{\substack{E_c < \epsilon_{\mathbf{k}'} \\ \epsilon_{\mathbf{k}n}^{(0)} - \epsilon_{\mathbf{k}'}^{\text{free}}}} \left[\psi_{\mathbf{k}n}^{(s)}(\mathbf{r}_1) \psi_{\mathbf{k}n}^{*(s)}(\mathbf{r}_2) - \psi_{\mathbf{k}n}^{(s)}(\mathbf{r}_1) \psi_{\mathbf{k}n}^{*(\bar{s})}(\mathbf{r}_2) \right] \times \frac{e^{i\mathbf{k}' \cdot (\mathbf{r}_2 - \mathbf{r}_1)}}{\epsilon_{\mathbf{k}n}^{(0)} - \epsilon_{\mathbf{k}'}^{\text{free}}}, \quad (27)$$

where in this last equation we have dropped the index n' and let \mathbf{k}' run over the extended Brillouin zone. $J_{\text{RKKY}}^{\text{free}}(\mathbf{r}_1, \mathbf{r}_2)$ is then a free-electron correction term that can be analytically integrated and that only depends on states below the Fermi energy and on the numerical value of E_c . In this way, instead of summing over a large number of bands, Eq. (25) only needs to be evaluated until convergence with respect to E_c is attained.

The wavefunctions $\psi_{\mathbf{k},n}^{(s)}(\mathbf{r}_j)$ required to calculate the interactions Eqs. (20)-(22) for both impurities were obtained from DFT calculations performed by using the VASP code⁴⁴⁻⁴⁶. The Pb (110) substrate was modeled as a periodic slab consisting of an 1×1 surface with N layers of Pb atoms and a vacuum layer of 15 Å to avoid coupling between surfaces in different periodic cells. Three top layers were allowed to relax while the other ones were kept fixed at their bulk lattice coordinates. Ionic forces were converged to be lower than 0.01 eV/Å, with a cutoff of 150 eV and using a Monkhorst-Pack⁴⁷ grid of $10 \times 10 \times 1$ k -points. All calculations were performed within the PAW method⁴⁸ and using PBEsol exchange-correlation functional⁴⁹. Since the interactions (20)-(22) are highly dependent on the accuracy of the wavefunctions $\psi_{\mathbf{k},n}^{(s)}(\mathbf{r}_j)$, a more stringent convergence condition and a larger number of empty bands were needed in their calculation. In order to obtain errors within 5% we used 120 empty bands and 1600 k -points. Calculations were performed with and without atomic spin-orbit interaction.

IV. RESULTS

A. Band Structure of Pb(110) and estimation of Rashba coupling parameter

The band structure of Pb(110) bulk and surface was first studied by Würde *et al*⁵⁰ using the empirical tight-binding method (ETBM) combined with the scattering-theory method to determine the different surface and resonant states. Given the large atomic number of Pb, the effect of the spin-orbit interaction cannot be neglected for this system, and needs to be taken into account. In the present work the Pb(110) band structure was obtained by self-consistent DFT calculations by including spin-orbit

coupling and by also considering relaxation effects on the (110) surface. In Figure 1 we show the calculated band structure for a Pb(110) slab with $N = 29$ layers. The surface and resonant states (red dots) are identified as those for which the sum of the square projections onto the top and bottom layers of the slab is greater than 30%. These results are in excellent agreement with the ETBM calculations of Würde *et al*. The large gap in the range between -6.5 to -4 eV corresponds to the marked energy difference between s and p levels in bulk Pb. Surface states (denoted as S_1 , S_2 and S_3 in Fig. 1) are mainly localized near the edges of the gaps arising along the X and Y directions, and extend between -2.4 and 3 eV. Bands S_1 and S_2 (S_3) consist mostly of p -states parallel (perpendicular) to the 110 surface. While the gap opening at point S for $E = -2$ eV is a consequence of spin-orbit coupling, the splitting of bands S_1 and S_2 arises from the Rashba shift at S, generated by the breaking of the symmetry along z . Indeed, by using the $\mathbf{k} \cdot \mathbf{p}$ approximation to fit bands S_1 and S_2 , it is possible to estimate the Rashba parameter to be $\alpha_R = 0.97 \text{ eV} \cdot \text{\AA}$.

The excellent agreement with the results by Würde *et al* justifies the use of the Kohn-Sham orbitals as the wavefunctions $\psi_{\mathbf{k},n}^{(s)}(\mathbf{r}_j)$ appearing in the expression of the unperturbed propagator Eq. (17) and in the calculation of the magnetic interactions Eqs. (20)-(22).

B. Convergence of the RKKY interaction

In order to ensure the convergence of the RKKY interaction with respect to the cutoff E_c , we evaluated the function $J_{\text{RKKY}}(\mathbf{r}_1, \mathbf{r}_2)$ as in Eq. (25). Since the magnitude of the correction term $J_{\text{RKKY}}^{\text{free}}(\mathbf{r}_1, \mathbf{r}_2)$ varies inversely with the distance between the two impurities, impurities located at larger distances would require smaller values of E_c in order to converge. For this reason the cutoff energy needs to be optimized for the minimum distance considered, which in our case corresponds to one half of the b lattice parameter (or, in other words, when $|\mathbf{r}_2 - \mathbf{r}_1| = 0.5b$). In Fig. 2 we display the total coupling $J_{\text{RKKY}} \equiv J_{\text{RKKY}}(0, 0.5b \hat{\mathbf{y}})$ together with $J^0 \equiv J_{\text{RKKY}}^0(0, 0.5b \hat{\mathbf{y}})$ and its correction $J^{\text{free}} \equiv J_{\text{RKKY}}^{\text{free}}(0, 0.5b \hat{\mathbf{y}})$, corresponding to a Pb(110) slab with $N = 11$ Pb layers for different values of the

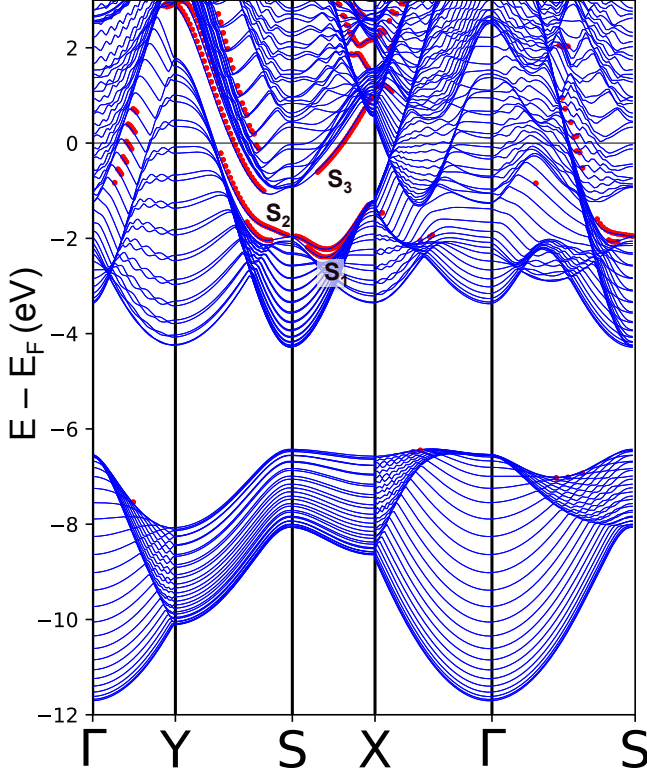


FIG. 1. (Color online) Calculated band structure for a 29-layer Pb(110) slab along high symmetry paths of the Brillouin zone. Surface and resonant states, represented by red dots, have been obtained by requiring the density for a given state projected onto the surface layers (top and bottom) be greater than 0.3. The surface states are labeled as S_1 , S_2 and S_3 .

cutoff energy E_c , taken with respect to E_F . Two observations become apparent in the plot. On the one hand, the slow decreasing rate of the correction terms (actually, oscillatory and analogous to the integral sin/cosine functions), which makes them impossible to neglect even for a very high energy cutoff. On the other hand, we observe that the correction closely compensates the variation of J^0 with respect to the cutoff. Despite the fact that for small values of E_c the free electron approximation is still too crude and the errors large, for values of E_c larger than $E_F + 20$ eV, the rate of variation of J^{free} clearly mirrors J^0 . In this last case, the total J_{RKKY} becomes flat and converges within a 2% of error. The same calculations were repeated for a $N=17$ -layer slab, obtaining a similar cutoff and the same values for J_{RKKY} (always within 2% error) as for the 11-layer case. In the light of these results and for the sake of simplicity, the rest of our calculations were performed for an 11-layer slab using a value $E_c = 22$ eV.

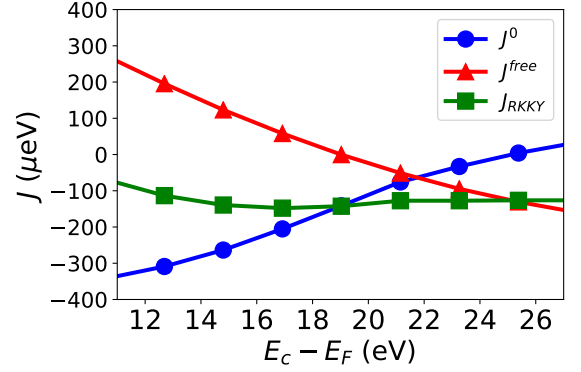


FIG. 2. (Color online) Convergence of the RKKY interaction J_{RKKY} (green squares) computed as in Eq. (25), as a function of the plane-wave cutoff energy $E_c - E_F$. Convergence is attained when the free-electron correction J^{free} (red triangles) exactly mirrors the uncorrected RKKY term J^0 (blue circles), for $E_c = 22$ eV above E_F .

C. Magnetic Interactions

As mentioned earlier, the free parameter J_K must be determined in order to compute the magnetic interactions in Eqs. (20)-(22). Here we estimated J_K by combining our DFT calculations with results from STM experiments studying the Kondo resonance in self-assembled metal-organic complexes (i.e., MnPc molecules) deposited on Pb(111)³⁹. In these experiments the weak character of the magnetic interactions between the adsorbed molecules is established by the close proximity of the measured subgap quasiparticle peaks (i.e., the “Shiba peaks”) to the superconducting gap. Furthermore, in these works the Kondo temperature T_K obtained from the Fano resonance near E_F ranges from 200 K to 400 K. If we consider an intermediate value $T_K \approx 300$ K, J_K can then be extracted from the Kondo temperature formula $k_B T_K = W e^{-1/\rho_{3D} J_K}$ ⁵¹. In this equation the value of the local density of states per unit volume at the Fermi level, ρ_{3D} , is obtained from DFT and corresponds to Pb’s located at the (110) surface. Within this model (which assumes a simplified rectangular flat band) the half bandwidth of the conduction states is calculated as $W = 1/(2\rho_{3D} V_{\text{atom}})$, with V_{atom} being the atomic volume for Pb. From this we obtain $\rho_{3D} = 0.01 \text{ eV}^{-1} \text{ \AA}^{-3}$ and $J_K = 10.80 \text{ eV} \cdot \text{\AA}^3$, thus yielding $\rho_{3D} J_K \approx 0.1$, which is consistent with our aforementioned assumption of weakly coupled adsorbates (such as MnPc on a Pb surface).

Once the parameter J_K has been obtained, the different magnetic interactions in Eqs. (20)-(22) were calculated as a function of distance for impurities located along the a and b directions on the Pb(110) surface. We considered two inequivalent positions for each impurity at the surface: either locating it halfway on the bridge between two Pb atoms of the top layer or above a Pb atom belonging to the layer immediately below [i.e. at $(0.5a, 0.5b)$]. In Fig. 3 we plot the RKKY, DM and

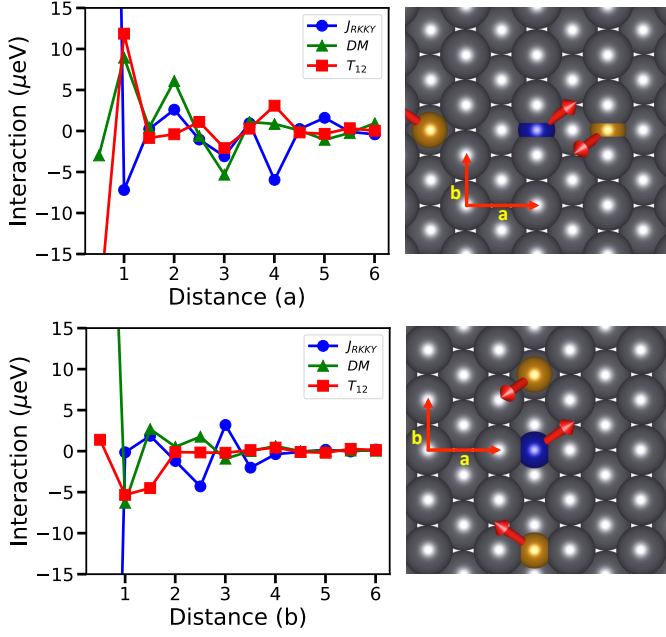


FIG. 3. (Color online) Top (Bottom): RKKY, DM and T_{12} magnetic interaction parameters for configurations with the reference impurity (blue) placed at the middle of the shorter (longer) bridge between two Pb atoms on the (110) surface and the second impurity (yellow) at $n.a/2$ ($n.b/2$) lattice parameters away along $a(b)$ -direction.

anisotropic-tensor (T_{12}) interactions locating a reference impurity at the bridge between two Pb's and letting the second impurity be located at either inequivalent position, in such a way that the distance between impurities is either an integer or half integer of one of the in-plane lattice parameters. Top and bottom panels in Fig. 3 display the calculated interactions for the reference impurity at a bridge location and the second impurity at different distances along the a and b directions, respectively. In Fig. 4 we repeated the calculations but this time locating the reference magnetic impurity at $(0.5a, 0.5b)$. In spite of the fact that all interactions follow the expected oscillatory behavior, their character departs significantly from the smooth and monotonic decay of the classical RKKY. It is also worth noticing the anisotropic character of the interactions: while we still encounter large peaks for impurities located 4 lattice parameters apart along a , interactions are significantly reduced for the same relative distance along b . This behavior, which at first glance may seem counterintuitive (since the impurities are at a closer distance along b), can be qualitatively understood by noticing that the flatter bands along a give rise to a larger density of states along this direction than along b , thus enhancing the magnitude of the interactions.

With the calculated magnetic interactions (J_{RKKY} , DM, T_{12}) it is then possible to search the spin configurations that minimize the effective Hamiltonian Eq. 19,

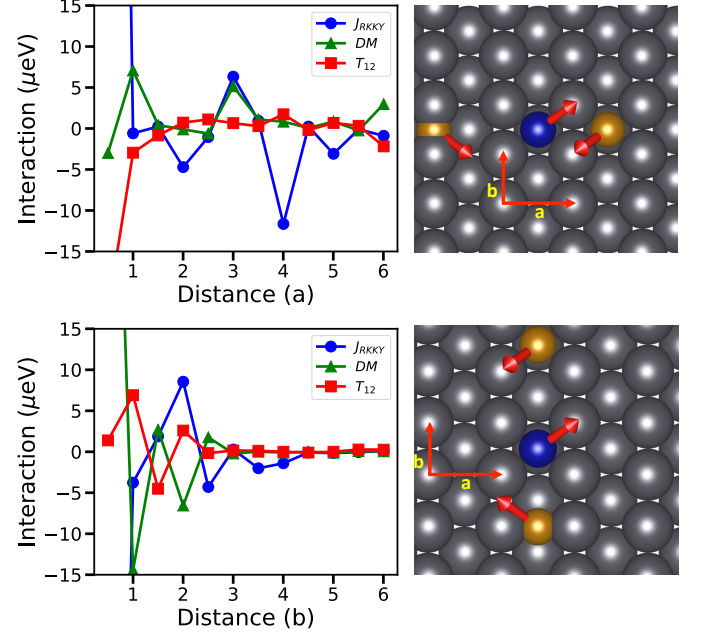


FIG. 4. (Color online) Top (Bottom): RKKY, DM and T_{12} magnetic interaction parameters for configurations with the reference impurity (blue) placed at $(0.5a, 0.5b)$ on the (110) surface and the second impurity (yellow) at $n.a/2$ ($n.b/2$) lattice parameters away along $a(b)$ -direction.

i.e., we can obtain the classical ground state configuration. In Fig. 5, top and bottom panels, we display these configurations together with their corresponding energies for interacting spins located at $\mathbf{r}_1 = (0.5a, 0.5b, 0)$ and $\mathbf{r}_2 = ((0.5 + n)a, 0.5b, 0)$, and at $\mathbf{r}_1 = (0.5a, 0.5b, 0)$ and $\mathbf{r}_1 = (0.5a, (0.5 + nb), 0)$, respectively. Taking for instance impurities one lattice parameter apart along the a direction, we see from Fig. 4 that in this case the dominant interaction is DM, thus favoring a canted spin configuration as the one shown in Fig. 5. Analogously, when the impurities are located two lattice parameters apart along the a direction, both DM and T_{12} interactions nearly vanish and the dominant interaction is RKKY, resulting in a collinear spin configuration, which since $J_{\text{RKKY}} < 0$ is ferromagnetic. Along the direction b , the behavior of magnetic ground state energy is approximately monotonic, and its value is abruptly reduced after $n = 3b$ and beyond. Contrarily, along the a direction the overall behavior is clearly not monotonic, and the magnetic energy-gain has a minimum at a distance $n = 4a$. This is a clear deviation from the RKKY interaction mediated by an idealized parabolic band.

Finally, we note that the order of magnitude of the interactions in Figs. 3, 4 and 5 are in agreement with recent experimental works on Fe atoms deposited on top of Pt(111)¹⁴.

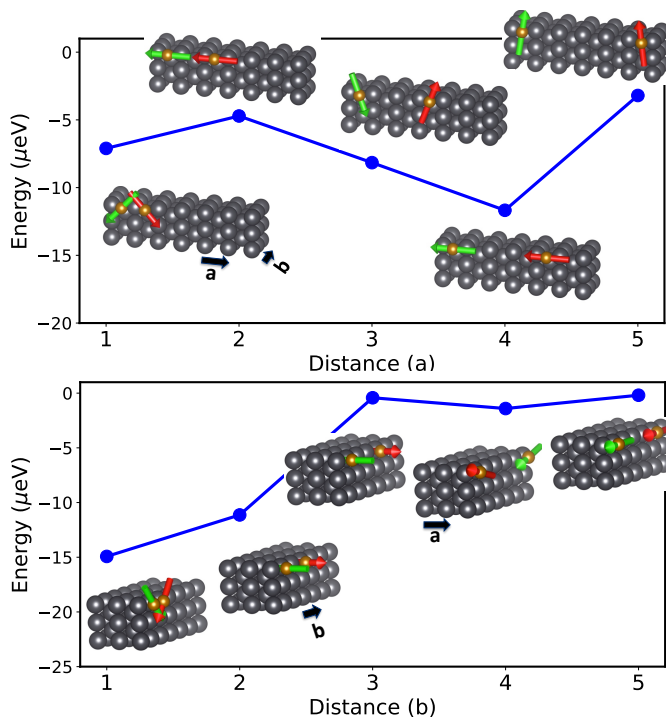


FIG. 5. (Color online) Top panel: Ground state energies and their corresponding spin configurations for the magnetic Hamiltonian of Equation 15 with a reference impurity (blue) located at $(0.5a, 0.5b)$ interacting with impurities (yellow) located at $(0.5na, 0.5b)$ on the Pb (110) surface. Bottom panel: Now the impurities interact along the \mathbf{b} -direction, i.e., the second impurity is placed at $(0.5a, 0.5nb)$.

V. SUMMARY AND CONCLUSIONS

We have investigated the indirect spin-spin interactions at the (110) surface of Pb, mediated by conduction electrons. Our study is motivated by the luring prospect of engineering spin-spin interactions in nanodevices with specific functionality at the surface of metals. In particular, the choice of Pb was motivated by its importance in experiments where superconductivity and strong spin orbit Rashba interactions (which emerge due to the lack of inversion symmetry at the surface) are combined. We have been able to estimate the Rashba parameter as $\alpha_R \approx 0.97 \text{ eV}\cdot\text{\AA}$.

In this work, assuming impurity spins \mathbf{S}_1 and \mathbf{S}_2 , weakly coupled to the Pb substrate via a generic s - d model (a situation that corresponds to a large class of experimental systems), we have developed a method which combines realistic *ab initio* calculations with low-cost computational effort. Using second-order perturbation theory and realistic DFT calculations for the electronic band structure of clean Pb(110), we have been able to systematically obtain the effective spin Hamiltonian between \mathbf{S}_1 and \mathbf{S}_2 at order J_K^2 with no additional assumptions. Since our method is perturbative, the underlying electronic structure of clean Pb(110) obtained within *ab*

initio is not modified. Technically, this means that the method, which is suitable for DFT band-structure calculations based on a periodic lattice, involves relatively small unit cells. This fact results in a considerable minimization of computational effort. It is worth mentioning that in general, the calculation of realistic nanoscale spin interactions through *ab initio* methods involve a great deal of computational effort (see, e.g. Ref. 57). Our method allows to systematically track the contribution of the conduction-electron propagators into the magnetic interaction functions [see Eqs. (20)-(22)]. In addition to the well-known RKKY interaction, the presence of Rashba spin-orbit coupling induces a finite DM and tensor matrix interactions, proportional α_R and α_R^2 , respectively. In particular the DM interaction is responsible for non-collinear magnetism and chiral effects (see Fig. 5, where we obtain non-collinear configurations from the minimization of the effective Hamiltonian). This type of interactions have been recently investigated in relation to Majorana proposals and skyrmion systems, which is currently investigated for magnetic storage technology.

The philosophy of our work is reminiscent to those of Imamura *et al*⁴³, Zhu *et al*⁵² and Bouaziz *et al*²⁶, where generic indirect magnetic interactions are obtained directly from the conduction electrons. However, in contrast to those works we have not assumed any specific model Hamiltonian for the conduction electrons. In that sense, this represents an important improvement since it allows to use the knowledge of realistic band structure calculations. We point out that in many cases where Rashba spin-orbit coupling is present, there is a tendency to use phenomenological 2D conduction band models^{26,43}. However, it is known that bulk electrons cannot be neglected and that they play an important role in, e.g., the Kondo effect⁵³⁻⁵⁵. A consequence of neglecting bulk electrons is the unrealistic slow decay of the RKKY and other indirect exchange interactions. In addition, in certain cases it has been identified that the presence of van Hove singularities in the idealized 2D band structure produce anomalous long-ranged interactions²⁶.

Being a perturbative approach based on the second-order expansion (the “RKKY approximation”), our method does not take into account higher-order scattering terms, and therefore is intrinsically limited to the weak coupling regime $\rho_{3D}J_K \rightarrow 0$. In that respect, extensions to include higher-order scattering terms have been proposed in the past^{26,56,57}. However, it is important to bear in mind that for a magnetic impurity in the strong-coupling regime, including higher-order scattering terms might not be enough, and also Kondo correlations, mixed-valence behavior, charge excitations, and other many-body effects should be addressed for a proper description. In that respect, Allerdt *et al*^{58,59} have recently considered many-body non-perturbative effects of the s - d exchange on the interaction by implementing quantum impurities at the surface of metals by implementing the density-matrix renormalization group (DMRG).

Another important conclusion of our work is the strong

anisotropy of the induced interactions depending on the directionality (a or b directions in Figs. 3 and 4), as a result of the symmetry of the Pb(110) surface. This result was also obtained theoretically⁵⁷ and experimentally¹² in different systems. In addition, the interaction is non-monotonic with the distance. These two aspects are in stark contrast with respect to the usually idealized parabolic-band RKKY.

Finally, we note that the band structure of Pb has been computed for the normal state, and that the superconducting gap in the spectrum of quasiparticle excitations of Pb has been ignored. We speculate that this approximation will not affect our results, as the superconducting effects should appear at distances of the order of the coherence length $\xi_{\text{Pb}} \approx 80$ nm, which are much larger than the interatomic distances in our calculations.

In summary, by combining *ab initio* methods with perturbation theory, we have studied the realistic indirect spin-spin interactions mediated by conduction electrons in the metallic surface of Pb(110). We speculate that this approach might be helpful in the design of weakly-coupled magnetic nanostructures with tailored interactions in order to obtain specific functionalities.

ACKNOWLEDGMENTS

The authors acknowledge financial support from PICT 2017-2081 (ANPCyT-Argentina). A.M.L. acknowledges financial support from PIP 11220150100364 (CONICET - Argentina) and Relocation Grant RD1158 - 52368 (CONICET - Argentina).

-
- * arebola@ifir-conicet.gov.ar
- ¹ M. A. Ruderman and C. Kittel, *Phys. Rev.* **96**, 99 (1954).
 - ² T. Kasuya, *Progress of Theoretical Physics* **16**, 45 (1956), <http://oup.prod.sis.lan/ptp/article-pdf/16/1/45/5266722/16-1-45.pdf>.
 - ³ K. Yosida, *Phys. Rev.* **106**, 893 (1957).
 - ⁴ M. N. Baibich, J. M. Broto, A. Fert, F. N. Van Dau, F. Petroff, P. Etienne, G. Creuzet, A. Friederich, and J. Chazelas, *Phys. Rev. Lett.* **61**, 2472 (1988).
 - ⁵ S. Doniach, *Physica B* **91**, 231 (1977).
 - ⁶ A. C. Hewson, *The Kondo Problem to Heavy Fermions* (Cambridge University Press, New York, 1993).
 - ⁷ H. v. Löhneysen, A. Rosch, M. Vojta, and P. Wölfle, *Rev. Mod. Phys.* **79**, 1015 (2007).
 - ⁸ E. Z. Meilikhov, *Phys. Rev. B* **75**, 045204 (2007).
 - ⁹ W. Dan and X. Shi-Jie, *Chinese Physics Letters* **25**, 1102 (2008).
 - ¹⁰ P. Wahl, P. Simon, L. Diekhöner, V. S. Stepanyuk, P. Bruno, M. A. Schneider, and K. Kern, *Phys. Rev. Lett.* **98**, 056601 (2007).
 - ¹¹ F. Meier, L. Zhou, J. Wiebe, and R. Wiesendanger, *Science* **320**, 82 (2008).
 - ¹² L. Zhou, J. Wiebe, S. Lounis, E. Vedmedenko, F. Meier, S. Blügel, P. H. Dederichs, and R. Wiesendanger, *Nature Physics* **6**, 187 (2010).
 - ¹³ A. A. Khajetoorians, J. Wiebe, B. Chilian, S. Lounis, S. Blügel, and R. Wiesendanger, *Nat. Phys.* **8**, 497 (2012).
 - ¹⁴ A. A. Khajetoorians, M. Steinbrecher, M. Ternes, M. Bouhassoune, M. dos Santos Dias, S. Lounis, J. Wiebe, and R. Wiesendanger, *Nature Communications* **7**, 10620 EP (2016), article.
 - ¹⁵ T. Esat, B. Lechtenberg, T. Deilmann, C. Wagner, P. Krüger, R. Temirov, M. Rohlfing, F. B. Anders, and F. S. Tautz, *Nat. Phys.* **12**, 867 (2016).
 - ¹⁶ S. Nadj-Perge, I. K. Drozdov, B. A. Bernevig, and A. Yazdani, *Phys. Rev. B* **88**, 020407 (2013).
 - ¹⁷ J. Klinovaja, P. Stano, A. Yazdani, and D. Loss, *Phys. Rev. Lett.* **111**, 186805 (2013).
 - ¹⁸ B. Braunecker and P. Simon, *Phys. Rev. Lett.* **111**, 147202 (2013).
 - ¹⁹ S. Nadj-Perge, I. K. Drozdov, J. Li, H. Chen, S. Jeon, J. Seo, A. H. MacDonald, B. A. Bernevig, and A. Yazdani, *Science* **346**, 602 (2014).
 - ²⁰ M. Ruby, F. Pientka, Y. Peng, F. von Oppen, B. W. Heinrich, and K. J. Franke, *Phys. Rev. Lett.* **115**, 197204 (2015).
 - ²¹ R. Pawlak, M. Kisiel, J. Klinovaja, T. Meier, S. Kawai, T. Glatzel, D. Loss, and E. Meyer, *npj Quantum Information* **2**, 16035 (2016).
 - ²² B. E. Feldman, M. T. Randeria, J. Li, S. Jeon, Y. Xie, Z. Wang, I. K. Drozdov, B. Andrei Bernevig, and A. Yazdani, *Nature Physics* **13**, 286 EP (2016), article.
 - ²³ N. Tsukahara, S. Shiraki, S. Itou, N. Ohta, N. Takagi, and M. Kawai, *Phys. Rev. Lett.* **106**, 187201 (2011).
 - ²⁴ *Surface Science* **630**, 343 (2014).
 - ²⁵ J. Girovsky, J. Nowakowski, M. E. Ali, M. Baljovic, H. R. Rossmann, T. Nijs, E. A. Aebys, S. Nowakowska, D. Siewert, G. Srivastava, C. Wäckerlin, J. Dreiser, S. Decurtins, S.-X. Liu, P. M. Oppeneer, T. A. Jung, and N. Ballav, *Nat. Commun.* **8**, 15388 (2017).
 - ²⁶ J. Bouaziz, M. dos Santos Dias, A. Ziane, M. Benakki, S. Blügel, and S. Lounis, *New Journal of Physics* **19**, 023010 (2017).
 - ²⁷ J. Linder and K. Halterman, *Phys. Rev. B* **90**, 104502 (2014).
 - ²⁸ J. Linder and J. W. A. Robinson, *Nature Physics* **11**, 307 (2015), review Article.
 - ²⁹ O. Krupin, G. Bihlmayer, K. Starke, S. Gorovikov, J. E. Prieto, K. Döbrich, S. Blügel, and G. Kaindl, *Phys. Rev. B* **71**, 201403 (2005).
 - ³⁰ P. Chuang, S.-C. Ho, L. W. Smith, F. Sfigakis, M. Pepper, C.-H. Chen, J.-C. Fan, J. P. Griffiths, I. Farrer, H. E. Beere, G. A. C. Jones, D. A. Ritchie, and T.-M. Chen, *Nature Nanotechnology* **10**, 35 (2014).
 - ³¹ S. Bandyopadhyay and M. Cahay, *Appl. Phys. Lett.* **85**, 1814 (2004).
 - ³² S. J. Frisken and D. J. Miller, *Phys. Rev. Lett.* **57**, 2971 (1986).
 - ³³ A. S. Oja, X. W. Wang, and B. N. Harmon, *Phys. Rev. B* **39**, 4009 (1989).
 - ³⁴ R. C. Patnaik, R. L. Hota, and G. S. Tripathi, *Phys. Rev. B* **58**, 3924 (1998).
 - ³⁵ B. Harmon, X.-W. Wang, and P.-A. Lindgård, *Journal of Magnetism and Magnetic Materials* **104-107**, 2113 (1992).

- ³⁶ P. Kim and J. H. Han, *Phys. Rev. B* **87**, 205119 (2013).
- ³⁷ A. Kundu and S. Zhang, *Phys. Rev. B* **92**, 094434 (2015).
- ³⁸ T. Kikuchi, T. Koretsune, R. Arita, and G. Tatara, *Phys. Rev. Lett.* **116**, 247201 (2016).
- ³⁹ K. J. Franke, G. Schulze, and J. I. Pascual, *Science* **332**, 940 (2011).
- ⁴⁰ B. W. Heinrich, L. Braun, J. I. Pascual, and K. J. Franke, *Nano Letters* **15**, 4024 (2015), pMID: 25942560, <http://dx.doi.org/10.1021/acs.nanolett.5b00987>.
- ⁴¹ J. W. Negele and H. Orland, *Quantum many particle systems* (Addison Wesley, Reading, 1987).
- ⁴² G. D. Mahan, *Many particle physics* (Plenum, New York, 1981).
- ⁴³ H. Imamura, P. Bruno, and Y. Utsumi, *Phys. Rev. B* **69**, 121303 (2004).
- ⁴⁴ G. Kresse and J. Hafner, *Phys. Rev. B* **47**, 558 (1993).
- ⁴⁵ G. Kresse and J. Furthmüller, *Computational Materials Science* **6**, 15 (1996).
- ⁴⁶ G. Kresse and J. Furthmüller, *Phys. Rev. B* **54**, 11169 (1996).
- ⁴⁷ H. J. Monkhorst and J. D. Pack, *Phys. Rev. B* **13**, 5188 (1976).
- ⁴⁸ G. Kresse and D. Joubert, *Phys. Rev. B* **59**, 1758 (1999).
- ⁴⁹ G. I. Csonka, J. P. Perdew, A. Ruzsinszky, P. H. T. Philipsen, S. Lebègue, J. Paier, O. A. Vydrov, and J. G. Ángyán, *Phys. Rev. B* **79**, 155107 (2009).
- ⁵⁰ K. Würde, A. Mazur, and J. Pollmann, *Phys. Rev. B* **49**, 7679 (1994).
- ⁵¹ A. C. Hewson, *The Kondo Problem to Heavy Fermions* (Cambridge University Press, Cambridge, 1993).
- ⁵² J.-J. Zhu, D.-X. Yao, S.-C. Zhang, and K. Chang, *Phys. Rev. Lett.* **106**, 097201 (2011).
- ⁵³ N. Knorr, M. A. Schneider, L. Diekhoner, P. Wahl, and K. Kern, *Phys. Rev. Lett.* **88**, 096804 (2002).
- ⁵⁴ M. A. Schneider, L. Vitali, N. Knorr, and K. Kern, *Phys. Rev. B* **65**, 121406 (2002).
- ⁵⁵ L. Limot and R. Berndt, *Applied Surface Science* **237**, 572 (2004), proceedings of the Seventh International Symposium on Atomically Controlled Surfaces, Interfaces and Nanostructures.
- ⁵⁶ P. Lloyd and P. Smith, *Advances in Physics* **21**, 69 (1972), <https://doi.org/10.1080/00018737200101268>.
- ⁵⁷ H. Ebert and S. Mankovsky, *Phys. Rev. B* **79**, 045209 (2009).
- ⁵⁸ A. Allerdtd, C. A. Büsser, G. B. Martins, and A. E. Feiguin, *Phys. Rev. B* **91**, 085101 (2015).
- ⁵⁹ A. Allerdtd, R. Žitko, and A. E. Feiguin, *Phys. Rev. B* **95**, 235416 (2017).